Geophysical Research Letters

RESEARCH LETTER
10.1029/2025GL118651

Ozone Trends in the Upper Troposphere-Lower Stratosphere Using Equivalent Latitude-Potential Temperature Coordinates

L. Millán[1], P. Hoor[2], M. I. Hegglin[3,4,5], G. L. Manney[6,7], P. S. Jeffery[8], F. M. Weyland[2], T. Leblanc[9], K. A. Walker[8], H. Boenisch[10], D. Kunkel[2], I. Petropavlovskikh[11], and H. Ye[4]

[1]Jet Propulsion Laboratory, California Institute of Technology, Pasadena, CA, USA, [2]Institute for Atmospheric Physics, University of Mainz, Mainz, Germany, [3]Institute of Climate and Energy Systems - Stratosphere (ICE-4), Forschungszentrum Jülich, Jülich, Germany, [4]Department of Meteorology, University of Reading, Reading, UK, [5]Institute for Atmospheric and Environmental Research, University of Wuppertal, Wuppertal, Germany, [6]NorthWest Research Associates, Socorro, NM, USA, [7]New Mexico Institute of Mining and Technology, Socorro, NM, USA, [8]Department of Physics, University of Toronto, Toronto, ON, Canada, [9]Jet Propulsion Laboratory, California Institute of Technology, Wrightwood, CA, USA, [10]Karlsruhe Institute of Technology, Institute of Meteorology and Climate Research, Karlsruhe, Germany, [11]Cooperative Institute for Research in Environmental Sciences, National Ocean and Atmospheric Administration, Boulder, CO, USA

Key Points:

- Equivalent latitude-potential temperature (EqL-θ) coordinates enhance robustness and interpretability of ozone trends, even at the tropics
- EqL-θ accounts for vortex variability when grouping ozone, whereas geographical coordinates ignore it, mixing polar and mid-latitude trends
- EqL-θ reveals statistically significant trends around the Antarctic vortex in the lower stratosphere, missed in geographical coordinates

Supporting Information:

Supporting Information may be found in the online version of this article.

Correspondence to:

L. Millán,
lmillan@jpl.nasa.gov

Citation:

Millán, L., Hoor, P., Hegglin, M. I., Manney, G. L., Jeffery, P. S., Weyland, F. M., et al. (2025). Ozone trends in the upper troposphere-lower stratosphere using equivalent latitude-potential temperature coordinates. *Geophysical Research Letters*, *52*, e2025GL118651. https://doi.org/10.1029/2025GL118651

Received 6 AUG 2025
Accepted 4 NOV 2025

Abstract We analyze ozone trends in the upper troposphere and lower stratosphere (UTLS, ~300–50 hPa), using geographical (latitude-pressure and latitude-altitude) and, for the first time, dynamical (equivalent latitude-potential temperature, EqL-θ) coordinates. Trends are determined using linear least squares fits, multiple linear regression, and dynamical linear modeling. Regardless of the method, EqL-θ improves consistency between trends across the UTLS, reduces large UT tropical uncertainties, alters the magnitude of mid-latitude trends, and, most notably, in the Southern polar lower stratosphere, reveals statistically significant trends exceeding 8% per decade during Antarctic Spring. This provides further evidence of Antarctic ozone recovery. These robust trends are not captured using geographical coordinates. We argue that EqL-θ enables more physically grounded interpretations of chemical ozone trends and their uncertainties, as EqL-θ accounts for the adiabatic (reversible) transport of ozone.

Plain Language Summary Ozone plays a vital role in Earth's atmosphere. In the stratosphere it protects life by blocking harmful ultraviolet (UV) radiation, while in the troposphere it acts as a powerful greenhouse gas and air pollutant. The region between these two layers, known as the upper troposphere and lower stratosphere (UTLS, ~10–22 km), is especially important because ozone in this region not only affects surface UV levels, but also climate and the quality of the air we breathe. Tracking ozone changes in this region is therefore essential for understanding its broader impacts. Typically, long-term changes of ozone (known as ozone trends) are determined using a geographical framework, where data are grouped by latitude and either altitude or pressure. In this study, we evaluate trends in these geographical frameworks and compare them to an alternative dynamical framework that accounts for the movement of ozone through the UTLS. We argue that this dynamical approach enables more physically grounded interpretations of ozone trends and their uncertainties. Notably, it reveals strong signals of Antarctic ozone hole chemical recovery that are not captured by commonly used geographical frameworks.

1. Introduction

Ozone, an essential atmospheric constituent, acts both as a protective shield by absorbing harmful ultraviolet radiation in the stratosphere (e.g., WMO, 2022) and a potent greenhouse gas in the troposphere (e.g., IPCC, 2021). Ozone in the upper troposphere and lower stratosphere (UTLS) is of particular interest due to its critical role in the Earth's radiation budget (e.g., Lacis et al., 1990; Riese et al., 2012), as well as its influence on air quality near the Earth's surface (e.g., Langford et al., 2015; Lin et al., 2015; Williams et al., 2019). Quantifying ozone trends in this region is thus essential for understanding its impacts not only for surface UV, but also on climate and air quality.

Despite decades of measurements from the ground, balloons, aircraft, and satellites, estimating ozone trends in the UTLS remains challenging because it is a transition region between the ozone-poor troposphere and the ozone-

rich stratosphere (e.g., Gettelman et al., 2011). UTLS ozone exhibits large spatio-temporal variability, primarily driven by dynamical fluctuations in the tropopause and the UTLS jets locations (e.g., Manney et al., 2011; Pan et al., 2009; Randel et al., 2007).

As part of the Observed Composition Trends And Variability in the UTLS (OCTAV-UTLS) Atmospheric Processes And their Role in Climate (APARC) activity, Millán et al. (2024) mapped multi-platform ozone data sets in various coordinate systems (including tropopause- and jet-relative coordinates) to systematically assess their influence on binned representations of ozone variability. They found that coordinate systems not aligned with transport barriers tend to overestimate ozone variability, as they fail to account for the shifting positions of jets and tropopauses or for wave-induced displacements of air parcels, thus inflating the binned variability. In contrast, equivalent latitude–potential temperature (EqL-θ) coordinates largely preserve ozone gradients at transport barriers and introduced the least binning-induced variability, yielding the smallest overall variability across the UTLS in all data sets and seasons (Millán et al., 2024). This is because EqL-θ relies on the conservation of potential temperature and potential vorticity (e.g., Hoskins, 1991; Krause et al., 2018), aligning well with the adiabatic (reversible) transport of ozone on timescale up to a few days.

We analyze ozone trends from 2005 to 2024 in the UTLS (~300–50 hPa) using data from the Aura Microwave Limb Sounder (MLS, Waters et al., 2006) and the Atmospheric Chemistry Experiment-Fourier Transform Spectrometer (ACE-FTS, Bernath et al., 2005). The data are binned in geographical coordinates (latitude-pressure and latitude-altitude) as well as in EqL-θ. To our knowledge, this is the first assessment of ozone trends using these dynamical coordinates. Tropopause and jet coordinates are not used because they are only suitable near their limited regions of influence (e.g., Hegglin et al., 2008; Millán et al., 2024). Unlike many studies that focus primarily on the LS above ~100 hPa, our analysis extends through the full depth of the LS and into the UT. We also conduct a global analysis rather than limiting the study to only extra-polar or polar regions.

2. Data Sets and Methods

We use Aura MLS version 5 (Schwartz, 2021) and ACE-FTS version 5.3 ozone data, applying their recommended quality screening (Livesey et al., 2022; Sheese et al., 2015). MLS ozone vertical resolution in the UTLS is around 3 km (Livesey et al., 2022) whereas ACE-FTS is around 1 km, achieved through oversampling in altitude (Hegglin et al., 2008). MLS provides about 3,500 profiles along the suborbital track every day during both day and night from 82°S and 82°N. In contrast, ACE-FTS measures one sunrise and one sunset per orbit, resulting in approximately 15 sunrise and 15 sunset occultations each day, largely concentrated at high latitudes. ACE-FTS achieves global coverage over a period of 3 months (i.e., one season), with almost identical coverage every year. Typical MLS and ACE-FTS sampling patterns are shown in Figures 1a and 1b. We use these data sets to exploit their overlapping long timeseries and to contrast the impact of using EqL-θ on dense versus coarse sampling. Both ozone data sets have been extensively validated (e.g., Hubert et al., 2016; Jiang et al., 2007; Sheese et al., 2017, 2022; Zou et al., 2024).

To map these ozone observations into different coordinate systems, we use the JEt and Tropopause Products for Analysis and Characterization (JETPAC) algorithms (e.g., Manney & Hegglin, 2018; Manney et al., 2011; Millán et al., 2023). JETPAC provides equivalent latitude, potential temperature, and characterization of tropopauses and UTLS jets, based on meteorological information from reanalysis fields for each measurement time and location. For this study, these fields are derived from the Modern-Era Retrospective analysis for Research and Applications, version 2 (MERRA-2, Gelaro et al., 2017). MERRA-2 has been extensively evaluated and is well-suited for UTLS studies (e.g., Homeyer et al., 2021; Manney et al., 2017; Tegtmeier et al., 2022), and shows no discontinuities (e.g., related to changes in assimilated observations or segmentation into multiple processing streams) during the study period (i.e., 2005 onward) (e.g., Fujiwara et al., 2017), either in temperature (i.e., θ, Long et al., 2017) or potential vorticity (i.e., EqL, Millán et al., 2021).

MLS and ACE-FTS ozone profiles are aggregated into seasonal zonal means in 5° bins (in either latitude or EqL). Vertically, the data are binned onto uniform grids using pressure (12 levels per decade), altitude (2 km spacing), or potential temperature (θ, 15 K spacing). For each grid cell time series (e.g., Figure 1c), trends are first calculated by applying a linear (least squares) fit to the deseasonaliazed data (Figure 1d). For these simple trend analyses, we avoid excluding sources of variability, such as El Niño Southern Oscillation (ENSO), the quasi-biennal oscillation (QBO), solar cycle, volcanic eruptions, etc, in the regression analysis to capture the full range of variability in ozone trends over the study period and to explore the impact of using EqL-θ without attributing other sources of

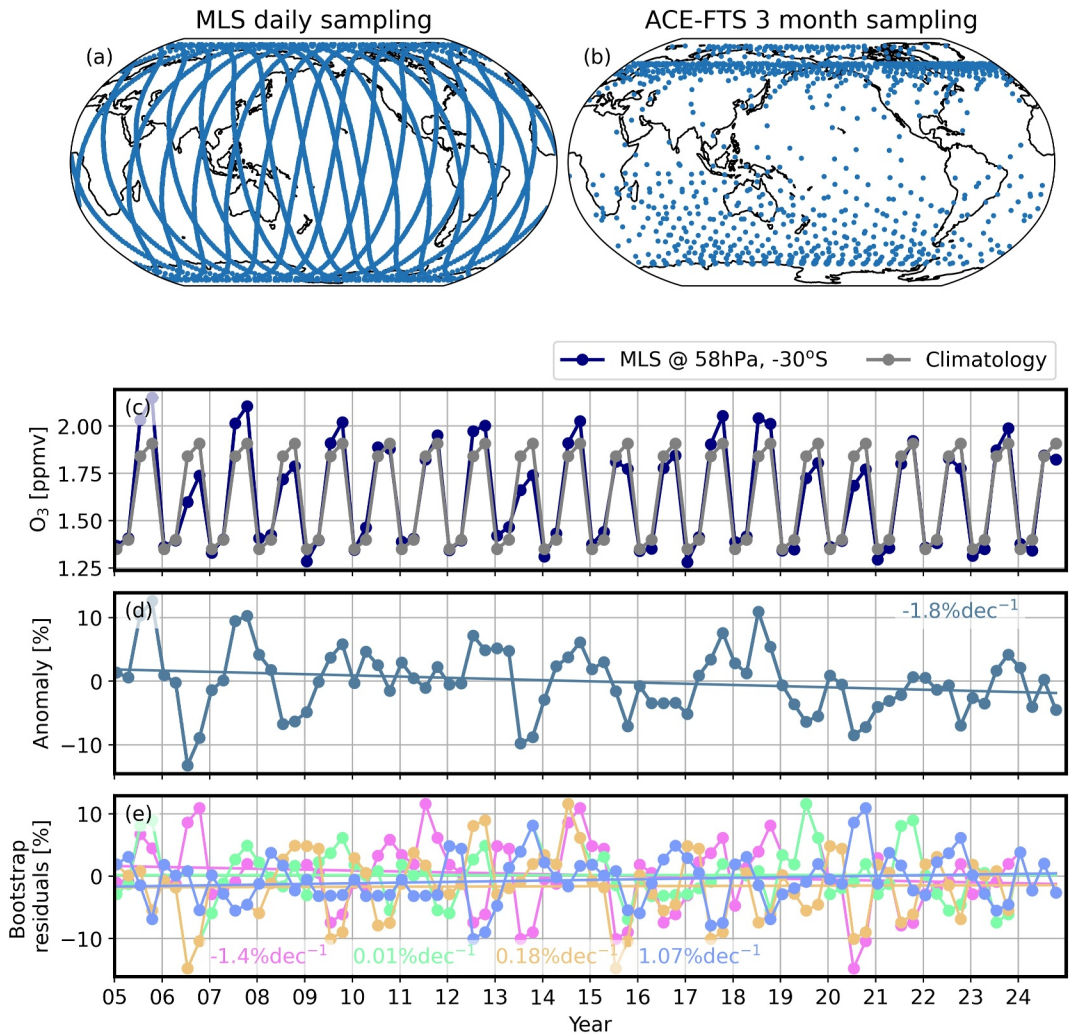

Figure 1. Example of (a) a Microwave Limb Sounder (MLS) daily sampling pattern and (b) an Atmospheric Chemistry Experiment-Fourier Transform Spectrometer 3-month (December-February) sampling pattern. (c) Example of an MLS ozone time series and climatology in one zonal bin. (d) Deseasonalized ozone anomalies. (e) Example bootstrapped residuals (i.e., anomalies−linear fit).

variability. Trends are computed only for timeseries in which at least 95% of the seasonal grid cells contain data points.

Uncertainties are estimated using a yearly block bootstrap resampling method (Figure 1e, e.g., Efron & Tibshirani, 1994), which accounts for autocorrelation in the residuals (e.g., Bourassa et al., 2014; Froidevaux et al., 2022). We report 2σ uncertainty values, that is, twice the standard deviations of the bootstrap distributions.

We further assess the impact of using EqL-θ instead of geographical coordinates by using more advanced trend methodologies (Section 5), namely multiple linear regression (MLR) and dynamical linear modeling (DLM). These approaches aim to disentangle the influence of major sources of variability (such as the solar cycle, QBO, ENSO) from long-term trends.

3. Linear Trends

MLS ozone trends (2005–2024) using the latitude-pressure coordinate system are shown in Figure 2a. For clarity, trends are discussed by regions as illustrated in Figure S1 in Supporting Information S1. In agreement with previous studies, the MLS trends suggest:

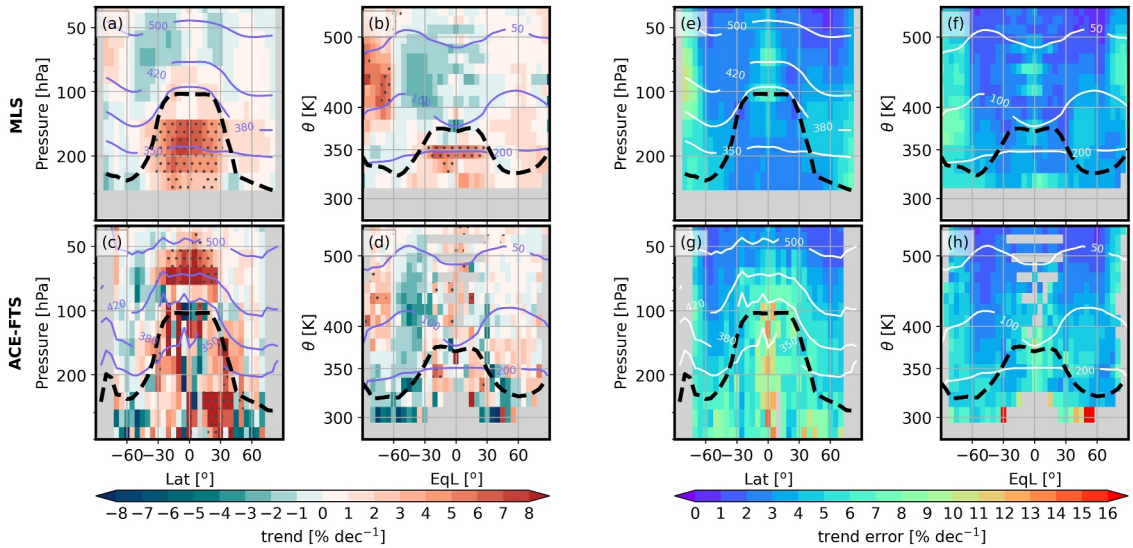

Figure 2. (a, b) Microwave Limb Sounder (MLS) and (c, d) Atmospheric Chemistry Experiment-Fourier Transform Spectrometer (ACE-FTS) ozone trends (2005–2024) using (a, d) latitude-pressure and (b, d) equivalent latitude-potential temperature. Gray regions indicate areas without measurements. The hatching represents statistical significance at the 2σ level. (e, f) MLS and (g, h) the ACE-FTS bootstrap 2σ trend uncertainties. Dashed black lines show the climatological WMO (thermal) tropopause. Contour lines show climatological potential temperature (in latitude-pressure panels) or pressure levels (in EqL-θ panels) as sampled by each instrument. Raggedness in the ACE-FTS panels arises from sparse sampling.

- Non-significant trends in the LS (∼100–50 hPa or ∼380–500 K) across tropical and mid-latitude regions (e.g., Godin-Beekmann et al., 2022; Petropavlovskikh et al., 2019; Steinbrecht et al., 2017; WMO, 2022).
- Statistically significant positive trends in the tropical UT (Froidevaux et al., 2025; Gaudel et al., 2024; Thompson et al., 2021).
- Positive (non-significant) trends in the Southern LS polar region (e.g., Johnson et al., 2023; Kuttippurath et al., 2018; Solomon et al., 2016; WMO, 2022).

Further, MLS data reveal a hemispheric asymmetry in the mid-latitude LS, with negative trends in the Southern hemisphere and near-zero ones in the Northern hemisphere. These results contrast with the trends reported by Godin-Beekmann et al. (2022), and WMO (2022), which were derived for the 2000–2020 period. A comparison with MLS ozone trends calculated over 2005–2020 (see Figure S2 in Supporting Information S1) suggests that this discrepancy might stem from the different start dates used in the analyses, as the MLS 2005–2020 trends continue to exhibit the asymmetry shown in Figure 2a.

MLS trends also show a hemispheric difference in the lowermost stratosphere (LMS, ∼200–100 hPa or ∼320–380 K), with negative trends in the Southern hemisphere and positive trends in the Northern one. Hemispheric asymmetries in stratospheric trace gas trends are well documented (e.g., Ball et al., 2018; Bognar et al., 2022; Mahieu et al., 2014; Strahan et al., 2020; Szeląg et al., 2020) and are generally associated with circulation changes (e.g., Dubé et al., 2025; Mahieu et al., 2014).

Figure 2c shows the latitude-pressure ACE-FTS ozone trends. Overall, there is limited consistency between trends derived using MLS and ACE-FTS, likely due to the sparse (non-uniform) ACE-FTS temporal and geographical sampling (Millán et al., 2016; Toohey et al., 2013). Further, ACE-FTS trends display potentially spurious positive trends in the tropical LS. For completeness, MLS and ACE-FTS trends using the latitude-altitude coordinate system are shown in Figure S3 in Supporting Information S1; results are similar to those for latitude-pressure, showing limited consistency between MLS and ACE-FTS trends. In latitude-altitude, MLS displays potentially spurious negative trends in the tropical LS (i.e., opposite in sign to those seen in ACE-FTS using pressure coordinates), highlighting the need for caution when interpreting results across these two coordinate systems. Note that the native vertical retrieval grids for ACE-FTS and MLS are altitude and pressure, respectively.

Ozone trends in EqL-θ coordinates show substantially better consistency between MLS (Figure 2b) and ACE-FTS (Figure 2d), despite their dissimilar sampling patterns, compared to trends in geographical coordinates. The most

prominent feature revealed by using EqL-θ is for trends in the Southern polar LS: inconsistent trends in latitude-pressure of ∼2% per decade for MLS (and −2% per decade for ACE-FTS) are revealed in EqL-θ as consistently positive trends of up to 5% per decade, with statistically significant trends in MLS just poleward of 60°S. Using EqL-θ ensures that the low ozone values arising from chemical depletion in the vortex are binned together even when the vortex is displaced/distorted, whereas geographical coordinates do not account for the air mass history and dynamical separation, thus misrepresenting both polar and mid-latitude ozone trends. The advantages of dynamical coordinate systems, particularly those accounting for the vortex, over conventional approaches have been highlighted by previous studies (e.g., Manney et al., 1995, 2023; McIntyre & Palmer, 1983; Schoeberl et al., 1992).

EqL-θ also improves the consistency between MLS and ACE-FTS mid-latitude trends. In the Southern mid-latitude LS, both data sets indicate stronger negative trends when using EqL-θ, increasing in magnitude from approximately −1.5% per decade in geographical coordinates to around −3.5% per decade.

Further, EqL-θ reveals more realistic ACE-FTS trends in the tropics, particularly a reduction in potentially spurious positive trends in the LS. However, even using EqL-θ, tropical trends derived from MLS and ACE-FTS remain inconsistent. MLS suggests mostly negative trends in the LS (consistent with previous studies, e.g., Benito-Barca et al., 2025; Dietmüller et al., 2021) whereas ACE-FTS indicates positive trends. This discrepancy likely reflects persistent limitations arising from sparse and seasonally biased ACE-FTS tropical sampling. A dedicated study of the impact of sampling biases upon trends would be valuable to fully address this issue.

The bootstrap 2σ trend uncertainties for MLS and ACE-FTS using latitude-pressure and EqL-θ are shown in Figures 2e, 2f and 2g, 2h, respectively. Using EqL-θ yields better consistency between the MLS and ACE-FTS trend uncertainties than using conventional geographical coordinates. For example, the large UT tropical trend uncertainties displayed in the ACE-FTS analysis are substantially reduced (from up to ∼12% to mostly less than 5% per decade) when using EqL-θ. Moreover, in the polar LS, when using EqL-θ, both data sets show trend uncertainties that more effectively capture the interannual variability associated with Antarctic and Arctic vortex-related chemical depletion. In contrast, when using traditional geographical coordinates, this variability signature is largely absent in the ACE-FTS analysis (due to its sparse sampling) and limited to the Southern hemisphere around 80 hPa in the MLS analysis.

4. Seasonal Dependence

Seasonal trends offer further insight into the role of dynamical variability in stratospheric ozone changes (e.g., Szeląg et al., 2020). In this analysis, the trends were determined using deseasonalized data from either December–February (DJF), March–May (MAM), June–August (JJA), or September–November (SON). That is, instead of applying a single linear fit to the 20-year time series containing 80 data points (20 years × 4 seasons), the data were divided into four separate seasonal time series, each consisting of 20 data points.

Figures 3a–3d and 3e–3h show the MLS and ACE-FTS seasonal trends, respectively, using latitude-pressure (Figure S4 in Supporting Information S1 shows the seasonal trends using latitude-altitude). Corresponding trends using EqL-θ are shown in Figures 3i–3p. In EqL-θ, seasonal features appear sharper, and consistency between the MLS and ACE-FTS trends improves substantially. For example, using EqL-θ mitigates artificially positive trends seen just above the tropical tropopause in the ACE-FTS analysis when using latitude-pressure (and artificially negative trends in MLS when using latitude-altitude). It also yields a more coherent representation of the ACE-FTS LMS trends. In the Southern LMS, trends are predominantly negative except during MAM, while in the Northern LMS, they are mostly positive except during DJF; matching the patterns seen in the MLS analysis.

The benefits of EqL-θ become even more pronounced in the polar LS. In both hemispheres, the imprint of the vortex on ozone trends is much more clearly captured by using EqL-θ. In the Southern Hemisphere, the Antarctic vortex becomes particularly evident in JJA (Figures 3i and 3m), during which season vortex-related chemical ozone loss begins. Statistically significant trends in JJA of ∼4% per decade are shown around the vortex edge (just poleward of 60°S) in both data sets. Although similar significant trends appear in geographical coordinates, ACE-FTS trends often show unrealistic localized values exceeding ∼8% per decade, likely arising from sampling impacts.

EqL-θ provides even more clarity in SON (Figures 3j and 3n), when rapid vortex chemical ozone loss occurs and minimum ozone values (along with maximum ozone hole depth and area) are reached. In this season, both data

10.1029/2025GL118651

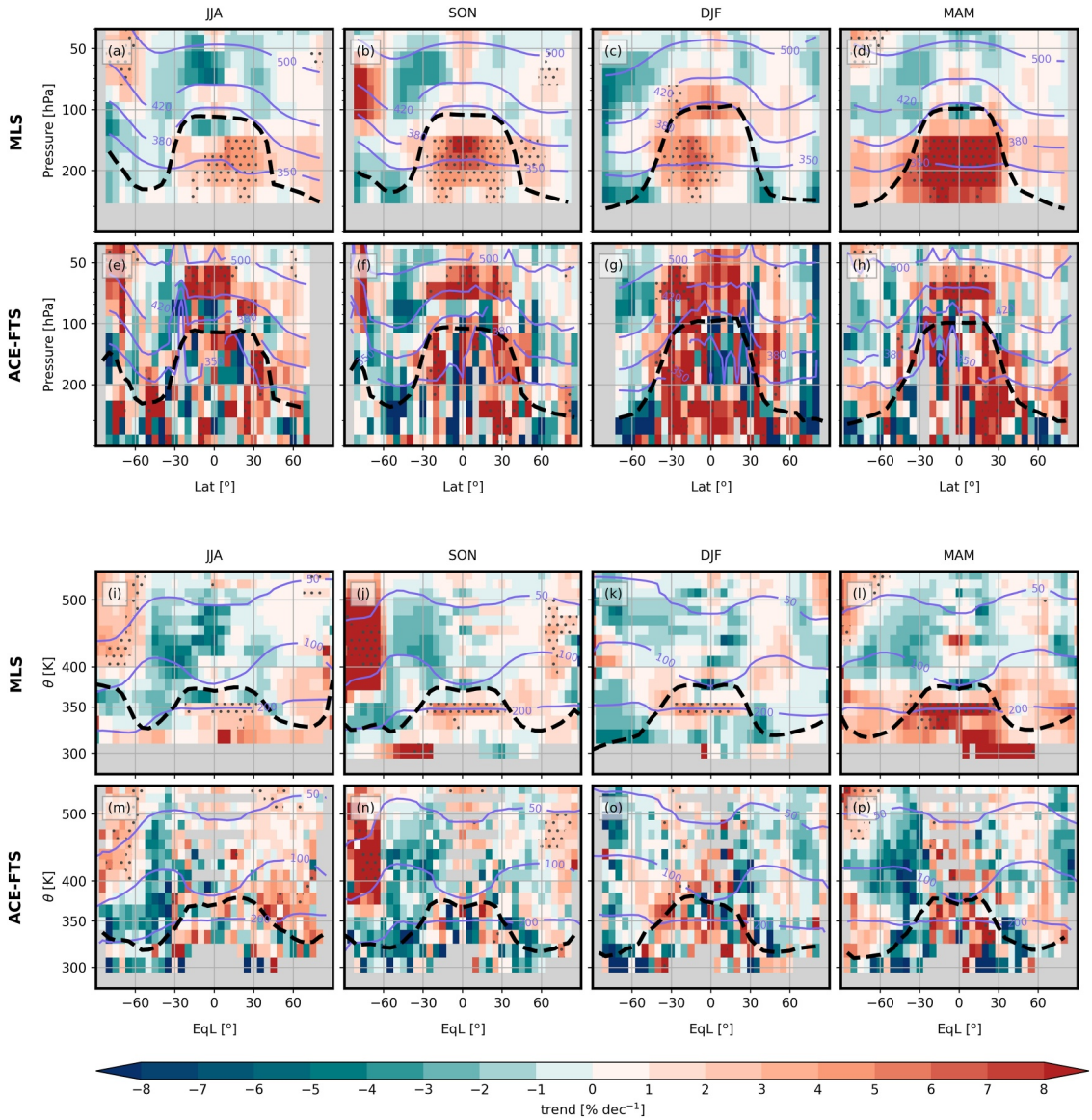

Figure 3. (a–d) Microwave Limb Sounder (MLS) and (e–h) Atmospheric Chemistry Experiment-Fourier Transform Spectrometer (ACE-FTS) seasonal ozone trends (2005–2024) using latitude-pressure. (i–l) MLS and (m–p) ACE-FTS seasonal ozone trends using EqL-θ.

sets show statistically significant positive trends in the entire Southern polar LS, with magnitudes exceeding ~8% per decade, suggesting a robust signal of ozone recovery, consistent with other recent analyses (e.g., Wang et al., 2025). Conversely, trends in geographical coordinates are not statistically significant and the ACE-FTS analysis even shows localized regions with negative trends.

Similar advantages emerge in the Arctic when using EqL-θ. In DJF (Figures 3k and 3o), which marks the onset of vortex-related ozone depletion in the Northern Hemisphere, MLS shows negative trends around the vortex edge and positive trends inside the vortex (a pattern also hinted at in ACE-FTS). During MAM (Figures 3l and 3p), when the Arctic experiences significant ozone depletion in some years, both data sets suggest negative trends (up to −6% per decade) across the polar LS region. In contrast, the Arctic vortex imprint is obscured in geographical coordinates because the Arctic vortex is virtually always distorted and displaced off the pole so that latitude-pressure binning "mixes up" mid-latitude and polar air (e.g., Arosio et al., 2024; Manney et al., 1995).

These results underscore the value of using a coordinate system that accounts for dynamics in trend analysis. EqL-θ reveals physically coherent trends in both data sets that are not captured by geographical coordinate

systems. Moreover, consistent with previous studies (e.g., Wang et al., 2025; Wargan et al., 2025), trends in EqL-θ provide statistically robust physically based evidence that the Antarctic ozone recovery is ongoing, despite the unusually low springtime ozone values reported in 2020–2023 (e.g., Kessenich et al., 2023; Yook et al., 2022).

Beyond the polar regions, the choice of coordinate system significantly influences the interpretation of ozone trends in the mid-latitude LS, even if the trends are non-significant. Using EqL-θ, Southern mid-latitudes show consistently stronger negative trends across all seasons while Northern mid-latitudes show predominantly positive trends during MAM and DJF and near-zero trends during JJA and SON. This seasonal pattern highlights the hemispheric asymmetry in mid-latitude LS ozone trends (i.e., negative trends in the Southern Hemisphere and positive trends in the Northern Hemisphere), consistent with analysis in Section 3. In contrast, trends in geographical coordinates are inconsistent: several LS regions in both hemispheres show spurious positive or negative trends, likely due to misclassification of polar air as mid-latitude air or vice-versa.

The bootstrap 2σ trend uncertainties associated to the trends shown in Figure 3 are shown in Figure S5 in Supporting Information S1. As with the full timeseries trends results, trend uncertainties when using EqL-θ are easier to interpret since they align with well-known sources of variability.

5. Advanced Regression Analysis

To further examine the impact of using EqL-θ instead of geographical coordinate systems, we compare trend results using MLR and DLM. MLR has been widely used for trend analysis (e.g., Froidevaux et al., 2019; Godin-Beekmann et al., 2022; Li et al., 2023; Nair et al., 2015; Olsen et al., 2019; Petropavlovskikh et al., 2019; Szeląg et al., 2020), whereas DLM is a newer technique (e.g., Laine et al., 2014), that has been used in recent trend studies because it can identify smoothly evolving, non-linear changes without requiring predefined inflection points (e.g., Ball et al., 2018; Weyland et al., 2025).

We use the publicly available MLR and DLM codes described by Petropavlovskikh et al. (2019) and Alsing (2019), respectively, with modifications to accommodate seasonal rather than monthly data. Both methods aim to disentangle the effects of dynamical, radiative, and solar processes on ozone trends. Specifically, we include proxies for the QBO, ENSO, stratospheric aerosol optical depth, and the 11-year solar cycle (see open research section for more details about these proxies).

MLR trend uncertainties are estimated by scaling the covariance measurement matrix to match the observed variance of the residuals. DLM uses an iterative process, based on Markov Chain Monte Carlo sampling, to infer possible time series from a Kalman filter framework. In particular, following an initial burn-in phase of 1,000 samples, each DLM run generates 2,000 model estimates of the system state, including a non-linear trend state time series. The DLM trend shown here corresponds to the mean difference in the non-linear trend state variable between 2005 and 2024, averaged across all samples. The standard deviation of this difference is used as the trend uncertainty estimate. DLM also incorporates observational uncertainties by accounting for the standard error of the mean at each grid cell throughout the time series.

The MLR and DLM full timeseries trend results are shown in Figures 4a–4h and 4i–4p for latitude-pressure and EqL-θ, and Figure S6 in Supporting Information S1 for latitude-altitude. These MLR and DLM results are broadly consistent with the linear least squares analysis results in Figure 2 and Figure S3 in Supporting Information S1, and support the conclusions drawn from the analysis in Section 3: all three methods demonstrate that using EqL-θ yields more reliable, consistent, and interpretable results when comparing MLS and ACE-FTS, especially in regions affected by complex dynamics such as the winter polar regions and near the tropopause.

That said, there are notable differences between the trend analyses (see Figures S7 and S8 in Supporting Information S1). Regardless of the coordinate system or data set used, trend magnitudes typically differ by $\sim\pm2\%$ per decade (i.e., $\pm100\%$ of the trend), but can vary by up to 7% per decade ($\sim500\%$) in the Northern Hemisphere LMS, by up to 4% per decade ($>500\%$) in the Northern polar LS, and by up to -6% per decade ($<100\%$) in the Southern polar LS. The Northern LMS and polar LS, in particular, show statistically significant positive trends in both the DLM and MLR analyses, but not in the simple linear regression.

Moreover, MLR uncertainties are consistently smaller than the bootstrap uncertainties derived for the linear least squares trends, differing by -1% to -4% per decade (-20% to -80%). DLM uncertainties are also generally smaller than the linear estimates by up to -4% per decade (-80%), but in the LMS they can exceed the linear

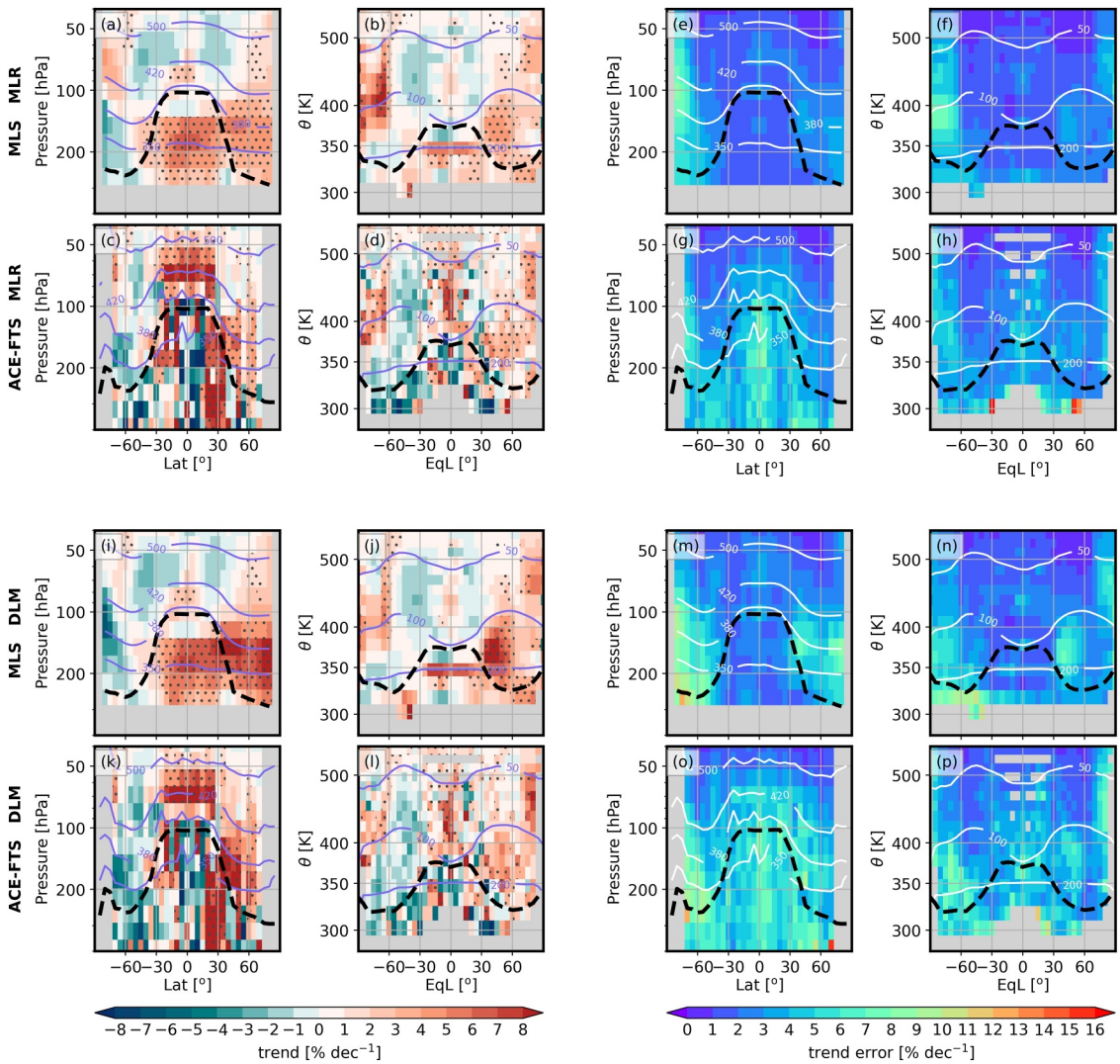

Figure 4. As Figure 2 using (a–h) multiple linear regression and using (i–p) DLM instead of a simple linear fit.

uncertainties by a similar magnitude (up to 4% per decade, or 80%). These differences (in magnitude and uncertainty) result in variations in the regions identified as statistically significant, both between different coordinate systems and different trend analysis methods.

Our results underscore the importance of interpreting trends not only using statistical significance, but also through consistency across data sets and methods, as well as a solid understanding of the underlying physical processes (e.g., Manney & Hegglin, 2018; Shepherd, 2021; Simmons, 2022). Analyzing trends in EqL-θ coordinates facilitates this informed interpretation of trend results by providing a framework that not only minimizes binning-induced variability (thus making results obtained from data sets with different sampling more comparable) but also grounds the analysis in a coordinate view that reflects the primary physical processes shaping the ozone distributions.

6. Conclusions

We have studied UTLS ozone trends from 2005 to 2024 using MLS and ACE-FTS data binned in geographic (latitude-pressure, latitude-altitude) and EqL-θ coordinates. To our knowledge, this is the first study of ozone trends using these dynamical coordinates. Trends are analyzed using deseasonalized data and three methods of

varying complexity: linear least squares fit, MLR, and dynamic linear model (DLM). Trends are analyzed globally rather than limiting the study to extra-polar or polar regions.

Using EqL-θ significantly improves the consistency between full timeseries trends derived from MLS and ACE-FTS, by accounting for transport-related variations, thus helping to mitigate the impact of different sampling. This is evident across all regions: In the Southern polar LS trends shift from 2% for MLS and −2% per decade for ACE-FTS to up to 5% per decade, with MLS data indicating statistical significance just poleward of 60°S. In mid-latitudes, EqL-θ helps prevent averaging of polar and extra-polar air masses, yielding clearer regional trends. In the tropics, it substantially mitigates spurious artifacts in the LS, particular those in latitude-pressure ACE-FTS trends and in latitude-altitude MLS trends.

Although the linear, MLR, and DLM trends exhibit similar overall patterns, the magnitudes and uncertainties can differ substantially. In particular, the Northern LMS and polar LS show statistically significant increasing trends in both the DLM and MLR analyses, but not in the simple linear regression.

Seasonal trends evaluated in EqL-θ highlight physically based patterns across regions. In the Antarctic, the influence of vortex-related chemical ozone depletion is clear in both data sets during the onset of the vortex-related chemical ozone loss (JJA) and during the period of rapid ozone depletion and minimum ozone values (SON), with statistically significant trends (exceeding 8% per decade) observed near the vortex edge. These results support the conclusion that Antarctic ozone recovery is ongoing. In contrast, using geographical coordinates, the vortex imprint remains confined to a narrower range, with trends that are no longer statistically significant.

In the Arctic, the vortex influence is more clearly resolved in DJF and MAM in EqL-θ (the periods when the Arctic may experience significant ozone depletion) than in geographical coordinate systems, although the trends remain non-significant in both coordinate systems. At mid-latitudes, coordinate choice strongly shapes the trend interpretation: EqL-θ reveals more consistent negative trends in the Southern Hemisphere and positive or near-zero trends in the Northern Hemisphere.

Independently of the trend methodology used, using EqL-θ better captures variability across the UTLS. It represents the Antarctic and Arctic chemical ozone loss more accurately, clarifies mid-latitude signals by accounting for vortex movement, and reduces large (spurious) tropical UT errors in the ACE-FTS analysis. Differences in uncertainty magnitudes across methods, and the resulting variation in statistically significant regions, underscore the need to interpret trends not solely by statistical significance but also via consistency across data sets and methods, supported by a solid understanding of underlying physical processes. By minimizing binning-induced variability, enhancing data set comparability, and aligning with the physical processes that control ozone distributions, EqL-θ provides a unified framework for assessing global ozone trends in the UTLS.

Conflict of Interest

The authors declare no conflicts of interest relevant to this study.

Data Availability Statement

The data sets used here are publicly available, as follows:

- Aura MLS Level 2 v5 data (Schwartz, 2021): https://doi.org/10.5067/Aura/MLS/DATA2516.
- ACE-FTS v5.3: https://databace.scisat.ca/level2/ace_v5.3.
- ACE-FTS error flags (Sheese & Walker, 2020): https://doi.org/10.5683/SP2/BC4ATC.
- ENSO proxy https://www.esrl.noaa.gov/psd/enso/mei/data/meiv2.data.
- QBO proxy https://acd-ext.gsfc.nasa.gov/Data_services/met/qbo/QBO_Singapore_Uvals_GSFC.txt.
- Solar proxy https://spdf.gsfc.nasa.gov/pub/data/omni/low_res_omni/omni2_all_years.dat.
- Aerosol proxy (GloSSAC v2.23) (Thomason, 2025): https://doi.org/10.5067/GLOSSAC-L3-V2.23.
- MERRA2 (Global Modeling and Assimilation Office (GMAO), 2015): https://doi.org/10.5067/WWQSXQ8IVFW8.

Acknowledgments
This research was supported by the ISSI in Bern through ISSI International Team Project 509. Work at the Jet Propulsion Laboratory, California Institute of Technology, was carried out under a contract with the National Aeronautics and Space Administration (80NM0018D 0004). GLM was supported by a JPL subcontract (1521127) and by NASA ACMAP/AST (Grant 80NSSC23K1007). PH and DK acknowledge support from the German Science Foundation through TRR 301 (428312742). FW was supported by HALO SPP 1294 (Grant HO-4225/19-1). IP was supported by a NOAA Cooperative Agreement (NA22OAR4320151) and NOAA Earth's Radiation Budget project. We thank M. Kovilakam for GloSSAC v2.23.

References

Alsing, J. (2019). dlmmc: Dynamical linear model regression for atmospheric time-series analysis. *Journal of Open Source Software*, *4*(37), 1157. https://doi.org/10.21105/joss.01157

Arosio, C., Chipperfield, M. P., Rozanov, A., Weber, M., Dhomse, S., Feng, W., et al. (2024). Investigating zonal asymmetries in stratospheric ozone trends from satellite limb observations and a chemical transport model. *Journal of Geophysical Research: Atmospheres*, *129*(8), e2023JD040353. https://doi.org/10.1029/2023jd040353

Ball, W. T., Alsing, J., Mortlock, D. J., Staehelin, J., Haigh, J. D., Peter, T., et al. (2018). Evidence for a continuous decline in lower stratospheric ozone offsetting ozone layer recovery. *Atmospheric Chemistry and Physics*, *18*(2), 1379–1394. https://doi.org/10.5194/acp-18-1379-2018

Benito-Barca, S., Abalos, M., Calvo, N., Garny, H., Birner, T., Abraham, N. L., et al. (2025). Recent lower stratospheric ozone trends in CCMI-2022 models: Role of natural variability and transport. *Journal of Geophysical Research: Atmospheres*, *130*(9), e2024JD042412. https://doi.org/10.1029/2024jd042412

Bernath, P. F., McElroy, C. T., Abrams, M. C., Boone, C. D., Butler, M., Camy-Peyret, C., et al. (2005). Atmospheric chemistry experiment (ACE): Mission overview. *Geophysical Research Letters*, *32*(15), L15S01. https://doi.org/10.1029/2005gl022386

Bognar, K., Tegtmeier, S., Bourassa, A., Roth, C., Warnock, T., Zawada, D., & Degenstein, D. (2022). Stratospheric ozone trends for 1984–2021 in the SAGE II–OSIRIS–SAGE III/ISS composite dataset. *Atmospheric Chemistry and Physics*, *22*(14), 9553–9569. https://doi.org/10.5194/acp-22-9553-2022

Bourassa, A. E., Degenstein, D. A., Randel, W. J., Zawodny, J. M., Kyrölä, E., McLinden, C. A., et al. (2014). Trends in stratospheric ozone derived from merged SAGE II and Odin-OSIRIS satellite observations. *Atmospheric Chemistry and Physics*, *14*(13), 6983–6994. https://doi.org/10.5194/acp-14-6983-2014

Dietmüller, S., Garny, H., Eichinger, R., & Ball, W. T. (2021). Analysis of recent lower-stratospheric ozone trends in chemistry climate models. *Atmospheric Chemistry and Physics*, *21*(9), 6811–6837. https://doi.org/10.5194/acp-21-6811-2021

Dubé, K., Tegtmeier, S., Ploeger, F., & Walker, K. A. (2025). Hemispheric asymmetry in recent stratospheric age of air changes. *Atmospheric Chemistry and Physics*, *25*(2), 1433–1447. https://doi.org/10.5194/acp-25-1433-2025

Efron, B., & Tibshirani, R. (1994). *An introduction to the bootstrap*. Chapman and Hall/CRC. https://doi.org/10.1201/9780429246593

Froidevaux, L., Kinnison, D. E., Gaubert, B., Schwartz, M. J., Livesey, N. J., Read, W. G., et al. (2025). Tropical upper-tropospheric trends in ozone and carbon monoxide (2005–2020): Observational and model results. *Atmospheric Chemistry and Physics*, *25*(1), 597–624. https://doi.org/10.5194/acp-25-597-2025

Froidevaux, L., Kinnison, D. E., Santee, M. L., Millán, L. F., Livesey, N. J., Read, W. G., et al. (2022). Upper stratospheric ClO and HOCl trends (2005–2020): Aura microwave limb sounder and model results. *Atmospheric Chemistry and Physics*, *22*(7), 4779–4799. https://doi.org/10.5194/acp-22-4779-2022

Froidevaux, L., Kinnison, D. E., Wang, R., Anderson, J., & Fuller, R. A. (2019). Evaluation of CESM1 (WACCM) free-running and specified dynamics atmospheric composition simulations using global multispecies satellite data records. *Atmospheric Chemistry and Physics*, *19*(7), 4783–4821. https://doi.org/10.5194/acp-19-4783-2019

Fujiwara, M., Wright, J. S., Manney, G. L., Gray, L. J., Anstey, J., Birner, T., et al. (2017). Introduction to the SPARC reanalysis intercomparison project (S-RIP) and overview of the reanalysis systems. *Atmospheric Chemistry and Physics*, *17*(2), 1417–1452. https://doi.org/10.5194/acp-17-1417-2017

Gaudel, A., Bourgeois, I., Li, M., Chang, K.-L., Ziemke, J., Sauvage, B., et al. (2024). Tropical tropospheric ozone distribution and trends from in situ and satellite data. *Atmospheric Chemistry and Physics*, *24*(17), 9975–10000. https://doi.org/10.5194/acp-24-9975-2024

Gelaro, R., McCarty, W., Suárez, M. J., Todling, R., Molod, A., Takacs, L., et al. (2017). The Modern-Era Retrospective analysis for Research and Applications, version 2 (MERRA-2). *Journal of Climate*, *30*(14), 5419–5454. https://doi.org/10.1175/jcli-d-16-0758.1

Gettelman, A., Hoor, P., Pan, L. L., Randel, W. J., Hegglin, M. I., & Birner, T. (2011). The extratropical upper troposphere and lower stratosphere. *Reviews of Geophysics*, *49*(3), RG3003. https://doi.org/10.1029/2011rg000355

Global Modeling and Assimilation Office (GMAO). (2015). Merra-2 inst3_3d_asm_nv: 3d, 3-hourly, instantaneous, model-level, assimilation, assimilated meteorological fields v5.12.4 [Dataset]. *Goddard Earth Sciences Data and Information Services Center (GES DISC)*. https://doi.org/10.5067/WWQSXQ8IVFW8

Godin-Beekmann, S., Azouz, N., Sofieva, V. F., Hubert, D., Petropavlovskikh, I., Effertz, P., et al. (2022). Updated trends of the stratospheric ozone vertical distribution in the 60 S–60 N latitude range based on the LOTUS regression model. *Atmospheric Chemistry and Physics*, *22*(17), 11657–11673. https://doi.org/10.5194/acp-22-11657-2022

Hegglin, M. I., Boone, C. D., Manney, G. L., Shepherd, T. G., Walker, K. A., Bernath, P. F., et al. (2008). Validation of ACE-FTS satellite data in the upper troposphere/lower stratosphere (UTLS) using non-coincident measurements. *Atmospheric Chemistry and Physics*, *8*(6), 1483–1499. https://doi.org/10.5194/acp-8-1483-2008

Homeyer, C. R., Manney, G. L., Millán, L. F., Boothe, A. C., Xian, T., Olsen, M. A., et al. (2021). Extratropical upper troposphere and lower stratosphere (ExUTLS). In M. Fujiwara, G. L. Manney, L. J. Grey, & J. S. Wright (Eds.), *S-rip final report (chap. 7)*. https://doi.org/10.17874/800dee57d13

Hoskins, B. J. (1991). Towards a PV-theta view of the general circulation. *Tellus A: Dynamic Meteorology and Oceanography*, *43*(4), 27–35. https://doi.org/10.3402/tellusa.v43i4.11936

Hubert, D., Lambert, J.-C., Verhoelst, T., Granville, J., Keppens, A., Baray, J.-L., et al. (2016). Ground-based assessment of the bias and long-term stability of 14 limb and occultation ozone profile data records. *Atmospheric Measurement Techniques*, *9*(6), 2497–2534. https://doi.org/10.5194/amt-9-2497-2016

IPCC. (2021). *Climate change 2021 – The Physical Science Basis: Working Group I contribution to the sixth assessment report of the Intergovernmental Panel on Climate Change*. Cambridge University Press. https://doi.org/10.1017/9781009157896

Jiang, Y. B., Froidevaux, L., Lambert, A., Livesey, N. J., Read, W. G., Waters, J. W., et al. (2007). Validation of Aura Microwave Limb Sounder ozone by ozonesonde and lidar measurements. *Journal of Geophysical Research*, *112*(D24), D24S34. https://doi.org/10.1029/2007jd008776

Johnson, B. J., Cullis, P., Booth, J., Petropavlovskikh, I., McConville, G., Hassler, B., et al. (2023). South pole station ozonesondes: Variability and trends in the springtime Antarctic ozone hole 1986–2021. *Atmospheric Chemistry and Physics*, *23*(5), 3133–3146. https://doi.org/10.5194/acp-23-3133-2023

Kessenich, H. E., Seppälä, A., & Rodger, C. J. (2023). Potential drivers of the recent large Antarctic ozone holes. *Nature Communications*, *14*(1), 7259. https://doi.org/10.1038/s41467-023-42637-0

Krause, J., Hoor, P., Engel, A., Plöger, F., Grooß, J. U., Bönisch, H., et al. (2018). Mixing and ageing in the polar lower stratosphere in winter 2015-2016. *Atmospheric Chemistry and Physics*, *18*(8), 6057–6073. https://doi.org/10.5194/acp-18-6057-2018

Kuttippurath, J., Kumar, P., Nair, P. J., & Pandey, P. C. (2018). Emergence of ozone recovery evidenced by reduction in the occurrence of Antarctic ozone loss saturation. *npj Climate and Atmospheric Science*, *1*(1), 42. https://doi.org/10.1038/s41612-018-0052-6

Lacis, A. A., Wuebbles, D. J., & Logan, J. A. (1990). Radiative forcing of climate by changes in the vertical distribution of ozone. *Journal of Geophysical Research*, *95*(D7), 9971–9981. https://doi.org/10.1029/jd095id07p09971

Laine, M., Latva-Pukkila, N., & Kyrölä, E. (2014). Analysing time-varying trends in stratospheric ozone time series using the state space approach. *Atmospheric Chemistry and Physics*, *14*(18), 9707–9725. https://doi.org/10.5194/acp-14-9707-2014

Langford, A. O., Pierce, R. B., & Schultz, P. J. (2015). Stratospheric intrusions, the Santa Ana winds, and wildland fires in Southern California. *Geophysical Research Letters*, *42*(14), 6091–6097. https://doi.org/10.1002/2015gl064964

Li, Y., Dhomse, S. S., Chipperfield, M. P., Feng, W., Bian, J., Xia, Y., & Guo, D. (2023). Quantifying stratospheric ozone trends over 1984–2020: A comparison of ordinary and regularized multivariate regression models. *Atmospheric Chemistry and Physics*, *23*(20), 13029–13047. https://doi.org/10.5194/acp-23-13029-2023

Lin, M., Fiore, A. M., Horowitz, L. W., Langford, A. O., Oltmans, S. J., Tarasick, D., & Rieder, H. E. (2015). Climate variability modulates western US ozone air quality in spring via deep stratospheric intrusions. *Nature Communications*, *6*(1), 7105. https://doi.org/10.1038/ncomms8105

Livesey, N. J., Read, W., Wagner, P. A., Froidevaux, L., Santee, M. L., Schwartz, M. J., et al. (2022). *Version 5.0x level 2 and 3 data quality and description document (tech. Rep. No. JPL D-105336 rev. B)*. Jet Propulsion Laboratory.

Long, C. S., Fujiwara, M., Davis, S., Mitchell, D. M., & Wright, C. J. (2017). Climatology and interannual variability of dynamic variables in multiple reanalyses evaluated by the SPARC reanalysis intercomparison project (S-RIP). *Atmospheric Chemistry and Physics*, *17*(23), 14593–14629. https://doi.org/10.5194/acp-17-14593-2017

Mahieu, E., Chipperfield, M. P., Notholt, J., Reddmann, T., Anderson, J., Bernath, P. F., et al. (2014). Recent northern hemisphere stratospheric HCl increase due to atmospheric circulation changes. *Nature*, *515*(7525), 104–107. https://doi.org/10.1038/nature13857

Manney, G. L., Froidevaux, L., Waters, J. W., & Zurek, R. W. (1995). Evolution of Microwave Limb Sounder ozone and the polar vortex during winter. *Journal of Geophysical Research*, *100*(D2), 2953–2972. https://doi.org/10.1029/94JD02823

Manney, G. L., & Hegglin, M. I. (2018). Seasonal and regional variations of long-term changes in upper-tropospheric jets from reanalyses. *Journal of Climate*, *31*(1), 423–448. https://doi.org/10.1175/jcli-d-17-0303.1

Manney, G. L., Hegglin, M. I., Daffer, W. H., Santee, M. L., Ray, E. A., Pawson, S., et al. (2011). Jet characterization in the upper troposphere/lower stratosphere (UTLS): Applications to climatology and transport studies. *Atmospheric Chemistry and Physics*, *11*(12), 6115–6137. https://doi.org/10.5194/acp-11-6115-2011

Manney, G. L., Hegglin, M. I., Lawrence, Z. D., Wargan, K., Millán, L. F., Schwartz, M. J., et al. (2017). Reanalysis comparisons of upper tropospheric–lower stratospheric jets and multiple tropopauses. *Atmospheric Chemistry and Physics*, *17*(18), 11541–11566. https://doi.org/10.5194/acp-17-11541-2017

Manney, G. L., Santee, M. L., Lambert, A., Millán, L. F., Minschwaner, K., Werner, F., et al. (2023). Siege in the southern stratosphere: Hunga Tonga-Hunga Ha'apai water vapor excluded from the 2022 antarctic polar vortex. *Geophysical Research Letters*, *50*(14), e2023GL103855. https://doi.org/10.1029/2023gl103855

McIntyre, M. E., & Palmer, T. N. (1983). Breaking planetary waves in the stratosphere. *Nature*, *305*(5935), 593–600. https://doi.org/10.1038/305593a0

Millán, L. F., Hoor, P., Hegglin, M. I., Manney, G. L., Boenisch, H., Jeffery, P., et al. (2024). Exploring ozone variability in the upper troposphere and lower stratosphere using dynamical coordinates. *Atmospheric Chemistry and Physics*, *24*(13), 7927–7959. https://doi.org/10.5194/acp-24-7927-2024

Millán, L. F., Livesey, N. J., Santee, M. L., Neu, J. L., Manney, G. L., & Fuller, R. A. (2016). Case studies of the impact of orbital sampling on stratospheric trend detection and derivation of tropical vertical velocities: Solar occultation vs. limb emission sounding. *Atmospheric Chemistry and Physics*, *16*(18), 11521–11534. https://doi.org/10.5194/acp-16-11521-2016

Millán, L. F., Manney, G. L., Boenisch, H., Hegglin, M. I., Hoor, P., Kunkel, D., et al. (2023). Multi-parameter dynamical diagnostics for upper tropospheric and lower stratospheric studies. *Atmospheric Measurement Techniques*, *16*(11), 2957–2988. https://doi.org/10.5194/amt-16-2957-2023

Millán, L. F., Manney, G. L., & Lawrence, Z. D. (2021). Reanalysis intercomparison of potential vorticity and potential-vorticity-based diagnostics. *Atmospheric Chemistry and Physics*, *21*(7), 5355–5376. https://doi.org/10.5194/acp-21-5355-2021

Nair, P. J., Froidevaux, L., Kuttippurath, J., Zawodny, J. M., Russell, J. M., Steinbrecht, W., et al. (2015). Subtropical and midlatitude ozone trends in the stratosphere: Implications for recovery. *Journal of Geophysical Research: Atmospheres*, *120*(14), 7247–7257. https://doi.org/10.1002/2014jd022371

Olsen, M. A., Manney, G. L., & Liu, J. (2019). The ENSO and QBO impact on ozone variability and stratosphere-troposphere exchange relative to the subtropical jets. *Journal of Geophysical Research: Atmospheres*, *124*(13), 7379–7392. https://doi.org/10.1029/2019jd030435

Pan, L. L., Randel, W. J., Gille, J. C., Hall, W. D., Nardi, B., Massie, S., et al. (2009). Tropospheric intrusions associated with the secondary tropopause. *Journal of Geophysical Research*, *114*(D10), D10302. https://doi.org/10.1029/2008jd011374

Petropavlovskikh, I., Godin-Beekmann, S., Hubert, D., Damadeo, R., Hassler, B., & Sofieva, V. (2019). SPARC/IO3C/GAW report on long-term ozone trends and uncertainties in the stratosphere. *SPARC*. https://doi.org/10.17874/F899E57A20B

Randel, W. J., Seidel, D. J., & Pan, L. L. (2007). Observational characteristics of double tropopauses. *Journal of Geophysical Research*, *112*(D7), D07309. https://doi.org/10.1029/2006jd007904

Riese, M., Ploeger, F., Rap, A., Vogel, B., Konopka, P., Dameris, M., & Forster, P. (2012). Impact of uncertainties in atmospheric mixing on simulated UTLS composition and related radiative effects. *Journal of Geophysical Research*, *117*(D16), D16305. https://doi.org/10.1029/2012jd017751

Schoeberl, M. R., Lait, L. R., Newman, P. A., & Rosenfield, J. E. (1992). The structure of the polar vortex. *Journal of Geophysical Research*, *97*(D8), 7859–7882. https://doi.org/10.1029/91jd02168

Schwartz, M. (2021). MLS/Aura level 2 ozone (O3) mixing ratio V005 [Dataset]. *NASA Goddard Earth Sciences Data and Information Services Center*. https://doi.org/10.5067/AURA/MLS/DATA2516

Sheese, P. E., Boone, C. D., & Walker, K. A. (2015). Detecting physically unrealistic outliers in ACE-FTS atmospheric measurements. *Atmospheric Measurement Techniques*, *8*(2), 741–750. https://doi.org/10.5194/amt-8-741-2015

Sheese, P. E., & Walker, K. (2020). Data quality flags for ACE-FTS level 2 version 4.1/4.2 data set [Dataset]. *Borealis*. https://doi.org/10.5683/SP2/BC4ATC

Sheese, P. E., Walker, K. A., Boone, C. D., Bernath, P. F., Froidevaux, L., Funke, B., et al. (2017). ACE-FTS ozone, water vapour, nitrous oxide, nitric acid, and carbon monoxide profile comparisons with MIPAS and MLS. *Journal of Quantitative Spectroscopy and Radiative Transfer*, *186*, 63–80. https://doi.org/10.1016/j.jqsrt.2016.06.026

Sheese, P. E., Walker, K. A., Boone, C. D., Bourassa, A. E., Degenstein, D. A., Froidevaux, L., et al. (2022). Assessment of the quality of ACE-FTS stratospheric ozone data. *Atmospheric Measurement Techniques*, *15*(5), 1233–1249. https://doi.org/10.5194/amt-15-1233-2022

Shepherd, T. G. (2021). Bringing physical reasoning into statistical practice in climate-change science. *Climatic Change*, *169*(1–2), 2. https://doi.org/10.1007/s10584-021-03226-6

Simmons, A. J. (2022). Trends in the tropospheric general circulation from 1979 to 2022. *Weather and Climate Dynamics*, *3*(3), 777–809. https://doi.org/10.5194/wcd-3-777-2022

Solomon, S., Ivy, D. J., Kinnison, D., Mills, M. J., Neely, R. R., & Schmidt, A. (2016). Emergence of healing in the Antarctic ozone layer. *Science*, *353*(6296), 269–274. https://doi.org/10.1126/science.aae0061

Steinbrecht, W., Froidevaux, L., Fuller, R., Wang, R., Anderson, J., Roth, C., et al. (2017). An update on ozone profile trends for the period 2000 to 2016. *Atmospheric Chemistry and Physics*, *17*(17), 10675–10690. https://doi.org/10.5194/acp-17-10675-2017

Strahan, S. E., Smale, D., Douglass, A. R., Blumenstock, T., Hannigan, J. W., Hase, F., et al. (2020). Observed hemispheric asymmetry in stratospheric transport trends from 1994 to 2018. *Geophysical Research Letters*, *47*(17), e2020GL088567. https://doi.org/10.1029/2020gl088567

Szeląg, M. E., Sofieva, V. F., Degenstein, D., Roth, C., Davis, S., & Froidevaux, L. (2020). Seasonal stratospheric ozone trends over 2000-2018 derived from several merged data sets. *Atmospheric Chemistry and Physics*, *20*(11), 7035–7047. https://doi.org/10.5194/acp-20-7035-2020

Tegtmeier, S., Krüger, K., Birner, T., Davis, N. A., Davis, S., Fujiwara, M., et al. (2022). Tropical troposphere layer. In M. Fujiwara, G. L. Manney, L. J. Grey, & J. S. Wright (Eds.), *S-rip final report (chap. 8)*. Retrieved from https://www.sparc-climate.org/wp-content/uploads/sites/5/2022/04/08_S-RIP_Report_Ch08.pdf

Thomason, L. W. (2025). Global space-based stratospheric aerosol climatology version 2.23 [Dataset]. *NASA Langley Atmospheric Science Data Center Distributed Active Archive Center*. https://doi.org/10.5067/GLOSSAC-L3-V2.23

Thompson, A. M., Stauffer, R. M., Wargan, K., Witte, J. C., Kollonige, D. E., & Ziemke, J. R. (2021). Regional and seasonal trends in tropical ozone from SHADOZ profiles: Reference for models and satellite products. *Journal of Geophysical Research: Atmospheres*, *126*(22), e2021JD034691. https://doi.org/10.1029/2021jd034691

Toohey, M., Hegglin, M. I., Tegtmeier, S., Anderson, J., Añel, J. A., Bourassa, A., et al. (2013). Characterizing sampling biases in the trace gas climatologies of the SPARC data initiative. *Journal of Geophysical Research: Atmospheres*, *118*(20), 11847–11862. https://doi.org/10.1002/jgrd.50874

Wang, P., Solomon, S., Santer, B. D., Kinnison, D. E., Fu, Q., Stone, K. A., et al. (2025). Fingerprinting the recovery of Antarctic ozone. *Nature*, *639*(8055), 646–651. https://doi.org/10.1038/s41586-025-08640-9

Wargan, K., Manney, G. L., & Livesey, N. J. (2025). Factors contributing to the unusually low Antarctic springtime ozone in 2020-2023. *Journal of Geophysical Research: Atmospheres*, *130*, e2025JD043621. https://doi.org/10.1029/2025JD043621

Waters, J. W., Froidevaux, L., Harwood, R. S., Jarnot, R. F., Pickett, H. M., Read, W. G., et al. (2006). The Earth Observing System Microwave Limb Sounder (EOS MLS) on the Aura satellite. *IEEE Transactions on Geoscience and Remote Sensing*, *44*(5), 1075–1092. https://doi.org/10.1109/TGRS.2006.873771

Weyland, F., Hoor, P., Kunkel, D., Birner, T., Plöger, F., & Turhal, K. (2025). Long-term changes in the thermodynamic structure of the lowermost stratosphere inferred from reanalysis data. *Atmospheric Chemistry and Physics*, *25*(2), 1227–1252. https://doi.org/10.5194/acp-25-1227-2025

Williams, R. S., Hegglin, M. I., Kerridge, B. J., Jöckel, P., Latter, B. G., & Plummer, D. A. (2019). Characterising the seasonal and geographical variability in tropospheric ozone, stratospheric influence and recent changes. *Atmospheric Chemistry and Physics*, *19*(6), 3589–3620. https://doi.org/10.5194/acp-19-3589-2019

WMO. (2022). Scientific assessment of ozone depletion: 2022.

Yook, S., Thompson, D. W. J., & Solomon, S. (2022). Climate impacts and potential drivers of the unprecedented Antarctic ozone holes of 2020 and 2021. *Geophysical Research Letters*, *49*(10), e2022GL098064. https://doi.org/10.1029/2022gl098064

Zou, J., Walker, K. A., Sheese, P. E., Boone, C. D., Stauffer, R. M., Thompson, A. M., & Tarasick, D. W. (2024). Validation of ACE-FTS version 5.2 ozone data with ozonesonde measurements. *Atmospheric Measurement Techniques*, *17*(23), 6983–7005. https://doi.org/10.5194/amt-17-6983-2024